Songklanakarin J. Sci. Technol.
40 (1), 79-86, Jan. - Feb. 2018

http://www.sjst.psu.ac.th

Original Article

Kinetics and control of palm fatty acid distillate esterification for a feasible biodiesel production

Apichat Saejio*, and Kulchanat Prasertsit

Department of Chemical Engineering, Prince of Songkla University, Hat Yai, Songkhla, 90112 Thailand

Received: 29 June 2016; Revised: 28 September 2016; Accepted: 17 October 2016

Abstract

The objective is to design the control structures for a smooth biodiesel production from palm fatty acid distillate. The kinetics of continuous esterification was investigated by considering the following operating parameters: reaction temperature in range of 50-70 °C and retention time in range of 10-30 min at a molar ratio of palm fatty acid distillate to methanol of 1:8. The experimental results gave the kinetic model as the pseudo-first order in free fatty acid for forward reaction and the second order in fatty acid methyl ester and water for backward reaction. The design and control of this process were studied also. Conventional and on-demand control structures with tray temperature control instead of composition control were proposed. Results showed that both proposed structures could handle changing in the process, ±10% of feed rate change, ±10°C of reactor temperature change, and 92-98% free fatty acid content with a satisfiable dynamic performance.

Keywords: biodiesel, esterification, kinetics, aspen plus, process control

1. Introduction

Biodiesel is an alternative fuel which is the product from the reaction between vegetable oil or animal fat and alcohol (e.g., methanol, and ethanol) with catalyst in suitable conditions (Chongkhong *et al.*, 2007; Lamaisri *et al.*, 2015; Van Gerpen *et al.*, 2004). Normally, transesterification reaction is chosen for biodiesel production since it is easier to operate than other processes (Zhang *et al.*, 2003; West *et al.*, 2008). However, this reaction requires oil containing very low free fatty acid (FFA) such as purified palm oil in order to prevent undesired product. If transesterification is carried out under alkali catalyst and high FFA content, saponification from FFA and the catalyst produces soap, which will inhibit the transesterification reaction. Consequently, it is difficult to separate biodiesel and glycerol (Chongkhong *et al.*, 2007; Jain *et al.*, 2011; Khan *et al.*, 2010). Since the raw material cost is the main production cost (Kapilakarn & Peugtong, 2007), using oil containing low FFA provides a high operating cost. Thus, purified palm oil is replaced by high FFA feed stocks such as palm fatty acid distillate (PFAD, a yellow solid at ambient temperature) by esterification reaction.

Esterification is the reaction between FFA and alcohol with the presence of acid catalyst to produce fatty acid methyl ester **(**FAME**)** or biodiesel and water as byproduct**.** The advantages of esterification are unlimited FFA content in feed stock, mild conditions, and low cost **(**Chongkhong *et al.*, 2007; Khan *et al.*, 2010; Yadav *et al.*, 2010**).** Furthermore, most of the FFA is converted to FAME, so the residual FFA and triglyceride is to be converted by the transesterification process**.**

To make a smooth biodiesel production, a control system is introduced to the process; however, to design a simple control system, the plant simulation requires all kinetic parameters**.** Therefore, the objectives of this investigation were to study the reaction kinetics of continuous esterification and to propose a feasible and smooth biodiesel production process from PFAD**.** Additionally, the conventional and on demand control structures were designed to maintain the process stability and biodiesel specification**.**

*Corresponding author
Email address: apichat.sj@hotmail.com

2. Materials

2.1 Chemicals

PFAD was obtained from Chumporn Palm Oil Industry Plc., Thailand. The PFAD mainly contained 93% of FFA, triglyceride, and impurities. Other chemicals used (Methanol, Sulfuric acid, and Sodium hydroxide) were commercial grade.

3. Experiment and Simulation

3.1 Continuous esterification process: Kinetic studies

The kinetics of esterification reaction from PFAD was studied. The main components of PFAD were recalculated and simplified as 53.75% palmitic acid, 39.25% oleic acid and 7% Triolein based on Chongkhong *et al.* (2007). Firstly, a preheated PFAD and 1.834 weight% of sulfuric acid based on PFAD in methanol solution were fed into the 0.57 L continuous-stirred tank reactor (CSTR). Operating parameters employed were reaction temperature in the range of 50-70°C and retention time in the range of 10-30 min at molar ratio of PFAD to methanol of 1:8 (Chongkhong *et al.*, 2007). Secondly, the product mixture after the reaction reached a steady state (4 times of reaction time) was sampled and poured into a separation funnel, and then allowed to settle into two phases for 1 hr. The bottom phase which was the FAME-rich phase was then washed, dehydrated, and analyzed for FFA compositions of the mixture employed AOCS Official Method Ca 5a-40 (The American Oil Chemists' Society, 1997). The FFA concentration profiles for each temperature after esterification were shown in Figure 1. (a). FFA reacted with methanol in the presence of sulfuric acid as catalyst to produce methyl ester and water as shown in Equation 1 by assuming that both FFA, palmitic and oleic acids, have the same reaction rate.

$$\text{FFA} + \text{Methanol} \underset{k_f}{\overset{k_b}{\leftrightarrow}} \text{Methyl ester} + \text{Water} \quad (1)$$

with k_f = forward reaction kinetic constant and k_b = backward reaction kinetic constant. Six kinetic models were proposed by Equations 2-7. The relative absolute error (RAE) equation as shown in Equation 8 was used instead of integral absolute error in order to achieve true magnitude of the quantity of error. In other words, it showed deviation of predicted values based on experimental or collected values. RAE was employed to find the suitable model and kinetic constants which shown in Table 1. The Table 1 indicates that Equation 5 gave the least RAE. Thus, this model was selected for simulation in the next part.

$$r = k_f [\text{FFA}] \quad (2)$$

$$r = k_f [\text{FFA}][\text{methanol}] \quad (3)$$

$$r = k_f [\text{FFA}] - k_b [\text{FAME}] \quad (4)$$

$$r = k_f [\text{FFA}] - k_b [\text{FAME}][\text{water}] \quad (5)$$

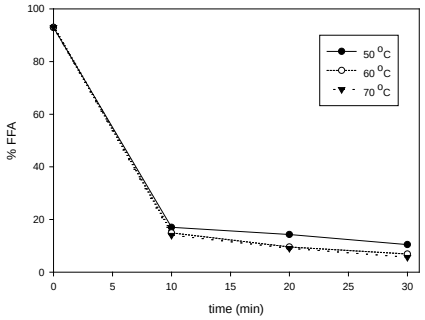

(a)

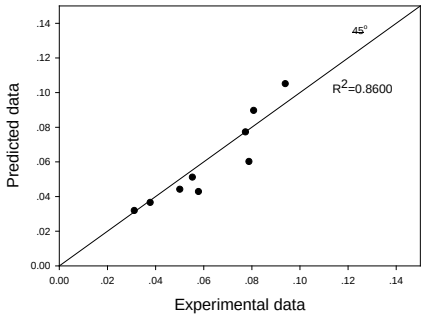

(b)

Figure 1. (a) Effect of temperature on FFA content after R1 and (b) Correlation plot for experimental data against predicted data from Equation 5.

Table 1. Kinetic parameters and relative absolute error of each model.

Model	A	E_a (kJ/mol)	A_-	E_{a-} (kJ/mol)	RAE
Eqs. (2)	6.47	18.772	-	-	1.1938
Eqs. (3)	0.61	18.781	-	-	1.0091
Eqs. (4)	6.47	18.772	1952.82	49.869	1.0176
Eqs. (5)	6.82	18.772	50.01	38.126	0.9742
Eqs. (6)	6.46	18.547	14.63	20.199	2.6799
Eqs. (7)	5.99	19.239	13.30	21.324	2.6675

$$r = k_f [\text{FFA}][\text{methanol}] - k_b [\text{FAME}] \quad (6)$$

$$r = k_f [\text{FFA}][\text{methanol}] - k_b [\text{FAME}][\text{water}] \quad (7)$$

$$\text{RAE} = \sum \left| \frac{exp - cal}{exp} \right| \quad (8)$$

with exp = experimental data or setpoint data and cal = calculated data or process data. This model shows that the forward reaction was pseudo-first order respected on FFA when methanol was excess corresponding to Yadav *et al.* (2010), and the backward reaction was second order respected on methyl ester, and water. The correlation plot described a comparison of predicted FFA content from Equation 5 with the experimental data is shown in Figure 1. (b). This demonstrates a good agreement of the model. The temperature dependent reaction rate constants for each reaction could be

expressed by the Arrhenius equation **(**Fogler, 2008**)** Equation 8**.**

$$k = A \exp(-E_a/RT) \quad (8)$$

with k = reaction rate constant, A = pre-factor, E_a = activation energy, and R the universal gas constant**.** Pre-factor and activation energy for each esterification reaction were shown in Table 1**.**

For reversible transesterification reaction **(**Issariyakul & Dalai, 2012; Prasertsit *et al.*, 2013**)** as shown in Equation 9, the residual 3**%** triolein, representing triglyceride, reacted with methanol in a present of sodium hydroxide as a catalyst to produce methyl ester and glycerol as a byproduct**.**

$$\text{Triolein} + 3\ \text{Methanol} \underset{k_b}{\overset{k_f}{\rightleftharpoons}} 3\ \text{Methyl oleate} + \text{Glycerol} \quad (9)$$

3.2 Process simulation

In the simulation, chemical components, chemical and physical properties, equilibrium data, and other calculations were complex. Therefore, the ASPEN PLUS V8.4, process simulator, was used to solve this complication. Because the polar components in the process were methanol and glycerol, Dortmund modified UNIFAC was one of the widely employed packages for calculating the activity coefficients of the components (Aspen Technology Inc., 2008; Simasatitkul *et al.*, 2013; Zhang *et al.*, 2003).

The biodiesel production models consisted of esterification reactor, transesterification reactor, neutralization reactor and methanol recovery columns**.** For esterification using kinetic parameters from the previous part, PFAD and 1.834 weight% of sulfuric acid based on PFAD in methanol were fed which optimum operating conditions that were a reaction temperature of 70 °C, retention time 60 min, and a molar ratio of PFAD to methanol 1:8 into the reactor (R1) (Chongkhong *et al.*, 2007) which FFA was converted to methyl ester. The excess methanol was recovered using the first distillation column (C1). Seven stages and 9.16 of a mass reflux ratio were required to achieve 99.5% of methanol purity in a recycle stream back into the R1. The esterified mixture was charged into the second reactor (R2) for neutralization. 3 M of Sodium hydroxide solution reacted with acid components; sulfuric acid and FFA were eliminated in this step. Neutralization was operated with excess sodium hydroxide for 80 °C and 15 min. The mixture of neutralization was separated by a decanter (Prasertsit *et al.*, 2014). The lighter phase was a FAME rich phase that was fed into the transesterification reactor (R3). In the transesterification reactor, triglyceride was reacted with methanol in a presence of sodium hydroxide catalyst. Since there was less triglyceride in the mixture (2-3%), and it easily convert to FAME, the 99% conversion of triolein in conversion reactor was assumed corresponding to Chongkhong *et al.* (2007). Moreover, the reversed reaction has a minor effect that can be neglect (Wenzel *et al.*, 2006). Operating conditions were reaction temperature of 80 °C, retention time 15 min, and 3.85 weight% of 0.396 M sodium hydroxide in methanol solution of feed stream (Chongkhong *et al.*, 2007). The second distillation column (C2) is necessary for the methanol recovery process. Seven stages and 3.11 of a mass reflux ratio were required to achieve 99.5% of methanol purity in recycle stream back into the transesterification reactor. The transesterified product was washed using 50°C of water in order to remove the impurities and undesired products. Finally, the washed FAME was flashed to remove water for meeting the biodiesel standard.

3.3 Process dynamics and control

In this section, the biodiesel process was designed a control structure: (1) Determining the manipulated variables, (2) Determining the temperature of the control tray, (3) Installing the controllers, (4) Using auto variation tuning to find the ultimate gain (K_u) and the ultimate period (P_u), and (5) Applying Tyreus–Luyben (TL) and Ziegler–Nichols (ZN) settings to find controller parameters (Luyben and Luyben, 1998; Hung *et al.*, 2010; Shen *et al.*, 2011).

3.3.1 Determining manipulated variables

PFAD, methanol and sulfuric acid were fed into the process. There are 35 manipulated variables. In this process that include 12 level controls; 3 pressure controls; 12 temperature controls; and 8 flow controls. The liquid levels were controlled by manipulating vessel inlet or outlet flow rate. For the the reactors, temperatures were controlled by the changing heat duty of the reactor. In esterification reactor, the fresh feed flow rates of methanol and sulfuric acid were manipulated to maintain the feed molar ratio of PFAD to methanol and a mass ratio of PFAD: sulfuric acid, respectively.

In the recovery process, the top distillation column pressure was controlled by manipulating condenser heat duty since vapor directly affected on the pressure. Tray temperature that was used instead of composition control of the methanol purity in recycle stream was controlled by reboiler heat duty for the reason that the temperature control gave fast and effective response. Because the first column reflux ratio had high value, the distillate flow rate was used to control a constant reflux ratio, and the reflux flow rate controlled a reflux drum level. While, second distillation column, the level of reflux drum was controlled by distillate flow rate, and the reflux flow rate was fixed (Luyben & Luyben, 1998). In neutralization reactor, feed ratio of esterified mixture: sodium hydroxide solution was maintained by manipulating sodium hydroxide solution flow rate. For water washing column, hot water was controlled to clean the FAME by manipulating hot water feed flow rate. Finally, vapor flow rate controlled the pressure of flash drum.

3.3.2 Control structure

Control structure I was designed according to Luyben and Luyben (1998) as shown in Figure 2(a). For this structure, the liquid outlet stream in each reactor controlled the liquid level of these reactors, and the fresh feed of PFAD controlled a biodiesel production rate. Control structure II was designed as shown in Figure 2(b). The bottom stream of flash drum was set on the demand of a product that was the production rate of biodiesel; flow controller was installed in

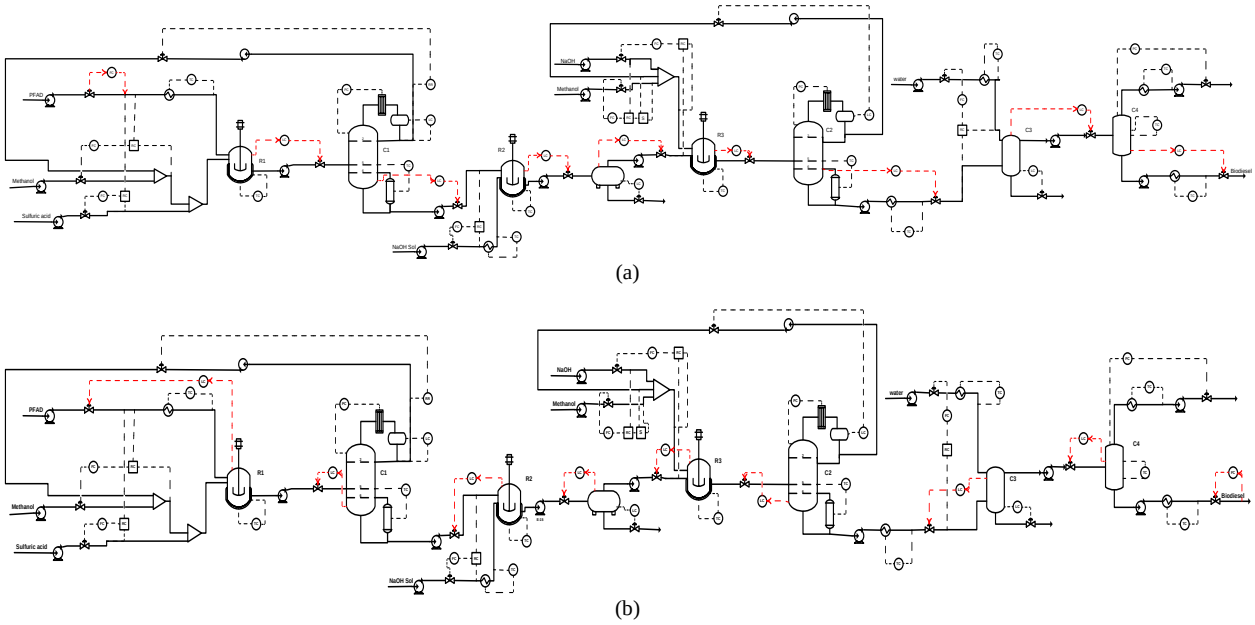

Figure 2. **(a)** Control structure I, **(b)** Control structure II**.**

this stream. The liquid level controls of units must be chosen to adapt backward form flash drum.

3.3.3 Selecting temperature control tray

One of several criteria for selecting temperature control tray is to look for a tray temperature in the distillation column at base case steady state conditions which has a large temperature change. The slope of temperature profiles of C1 and C2 indicated that were the steepest at a 5th stage of both columns as shown in Figure 3. Then, Figure 4(a) and (b) illustrated tray 5th of the both columns had largest temperature change when the reboiler duties of columns were changed. Therefore, they were selected to be a temperature control tray (Luyben, 2006; Luyben & Luyben, 1998).

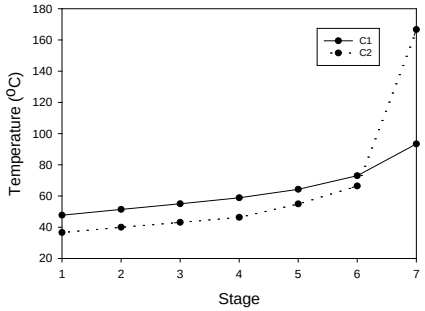

Figure 3. Temperature profiles of C1 and C2**.**

3.3.4 Setting controller

The controller structure was designed and simulated using Aspen Plus Dynamics. Proportional controllers were used for liquid level controls. Since its offset could be accepted, the tuning parameter of a level controller was

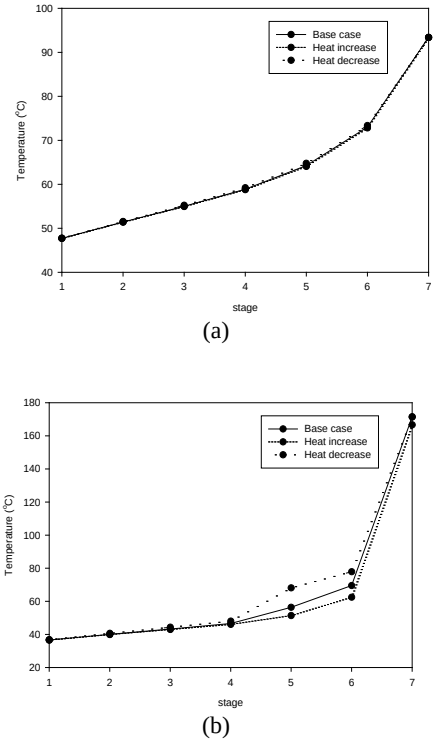

Figure 4. Effect of changes in column boilup temperature profile on (a) C1 and (b) C2.

K_c = 2. Level of reactor was impacted reaction rates; therefore, the higher gain value K_c = 10 was used. Flow, pressure, and temperature were controlled using the proportional integral controllers. The controller parameters of flow control should be moderate gain and a small integral time

Table 2. Temperature controller settings for control structure I.

Controlled variable	Manipulated variable	TL		ZN	
		K_c	τ_I (min)	K_c	τ_I (min)
PFAD feed	Heat duty	42.52	13.2	61.87	5
R1	Reactor duty	2.27	13.2	2.83	5
Tray 5th of C1	Reboiler duty	1.56	2.64	2.15	1.5
Sodium hydroxide feed to R2	Heat duty	3.29	13.2	18.1	1.5
R2	Reactor duty	7.51	13.2	10.97	5
R3	Reactor duty	90.08	13.2	135.11	5
Tray 5th of C2	Reboiler duty	3.21	18.48	4.39	7
Bottom stream of C2	Heat duty	7.51	2.64	13.0	1
Water feed to C3	Heat duty	8.59	7.92	15.14	3.5
C4	Heat duty	2.83	15.84	4.06	6.5
Bottom stream of C4	Heat duty	3.57	6.6	5.19	2.5
Top stream of C4	Heat duty	1.06	2.64	2.93	1

Table 3. Temperature controller settings for control structure II.

Controlled variable	Manipulated variable	TL		ZN	
		K_c	τ_I (min)	K_c	τ_I (min)
PFAD feed	Heat duty	42.52	13.2	61.85	5
R1	Reactor duty	2.44	11.88	3.53	4.5
Tray 5th of C1	Reboiler duty	3.89	2.64	5.53	1
Sodium hydroxide feed to R2	Heat duty	4.08	3.96	5.37	2.5
R2	Reactor duty	6.73	13.2	9.87	5
R3	Reactor duty	34.15	13.2	87.77	3.5
Tray 5th of C2	Reboiler duty	10.98	26.4	15.92	10
Bottom stream of C2	Heat duty	5.19	7.92	13.29	3
Water feed to C3	Heat duty	9.37	9.24	13.90	3
C4	Heat duty	2.68	15.84	3.96	6
Bottom stream of C4	Heat duty	3.53	6.6	5.10	2.5
Top stream of C4	Heat duty	0.70	3.96	3.83	2

were K_c = 0.5; and τ_I = 0.3 min because the dynamics of flow measurement were fast. For pressure control, Normal pressure controller parameters were K_c = 2; and τ_I = 10 min. Two first order models of 0.5 min time lag were assumed for measurement temperature (Luyben, 2002). For each temperature control loop, the ultimate gain and ultimate period obtained from auto tuning variation method, and controller parameters were computed by TL and ZN. The controller parameters of a piece controller were shown in Table 2 and 3 for conventional and on demand control structures, respectively.

3.3.5 Robustness

Control robustness was tested for each control structure by increasing small percentage until it became uncontrollable. The results show the control robustness were ±10% of PFAD feed flow rate for control structure I or ±10% of biodiesel production rate for control structure II, ±10°C of esterification reactor temperature and 92%-98% of FFA content in PFAD feed stream. Figure 5 to 7 and Figure 8 to 10 were temperature dynamic responses for control structure I and II, respectively. The results indicated that the ZN tuning method had less overshoot than TL tuning method. However, these two setting methods have no significant difference in RAE value as shown in Table 4, and they can be used to tune the controllers for biodiesel production process because the process is unlikely to fluctuate. In addition, the two proposed structures could eliminate interferences or disturbance, and biodiesel specification of all robustness tests still achieved the

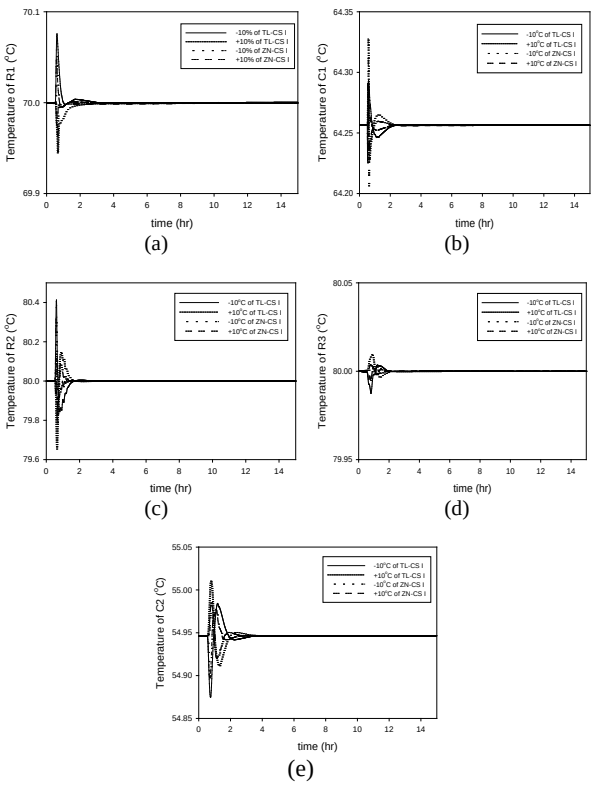

Figure 5. Temperature dynamic responses of TL and ZN-tuned control structure I for PFAD feed rate change.

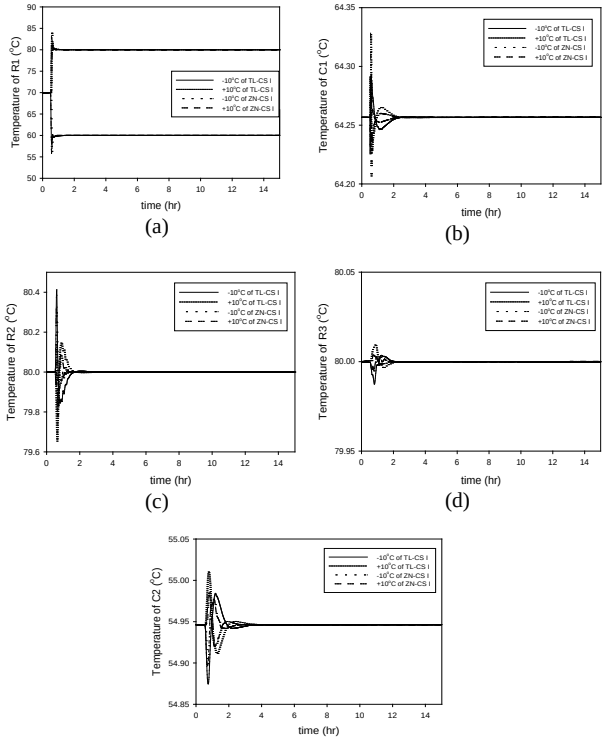

Figure 6. Temperature dynamic responses of TL and ZN-tuned control structure I for R1 temperature change.

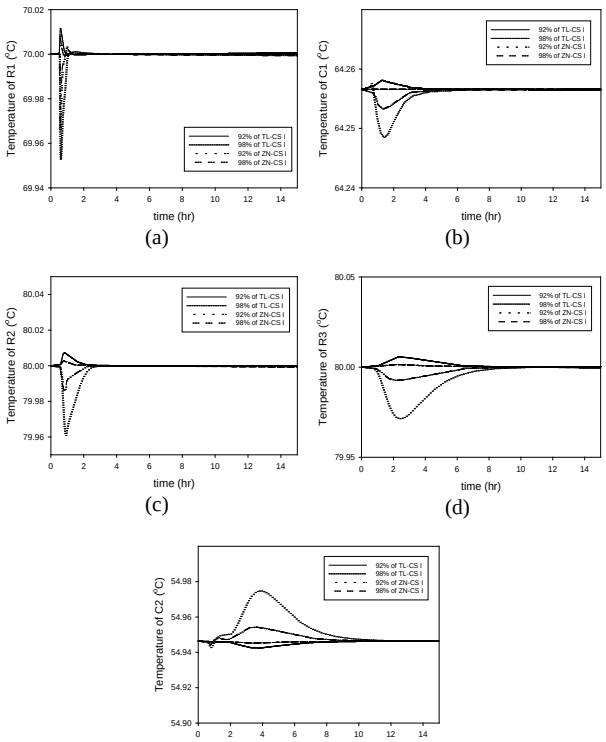

Figure 7. Temperature dynamic responses of TL and ZN-tuned control structure I for FFA in PFAD change.

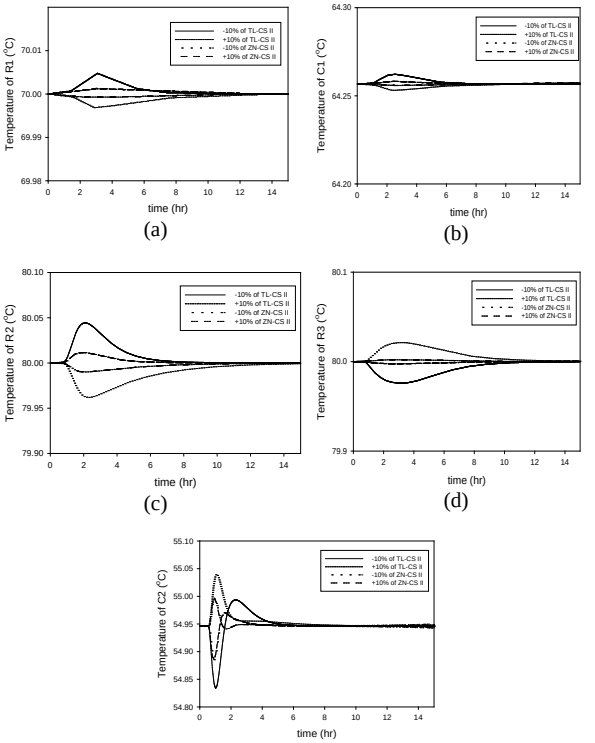

Figure 8. Temperature dynamic responses of TL and ZN-tuned control structure II for production rate change.

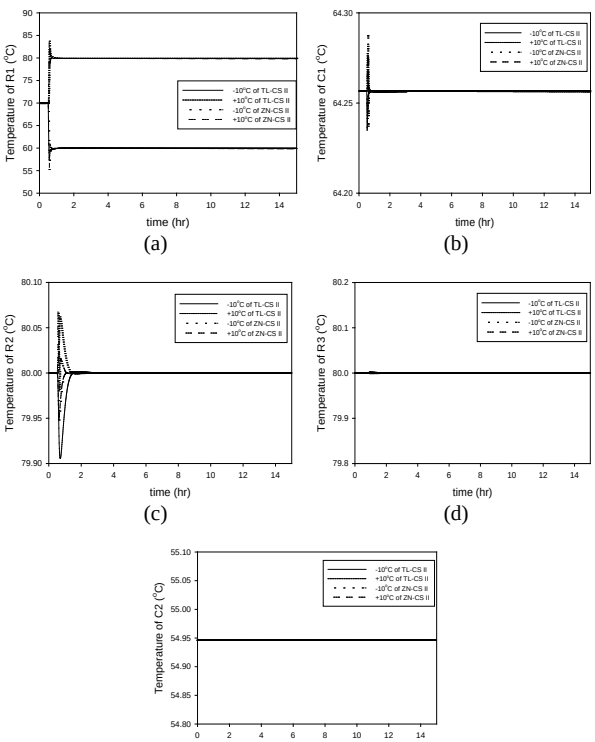

Figure 9. Temperature dynamic responses of TL and ZN-tuned control structure II for R1 temperature change.

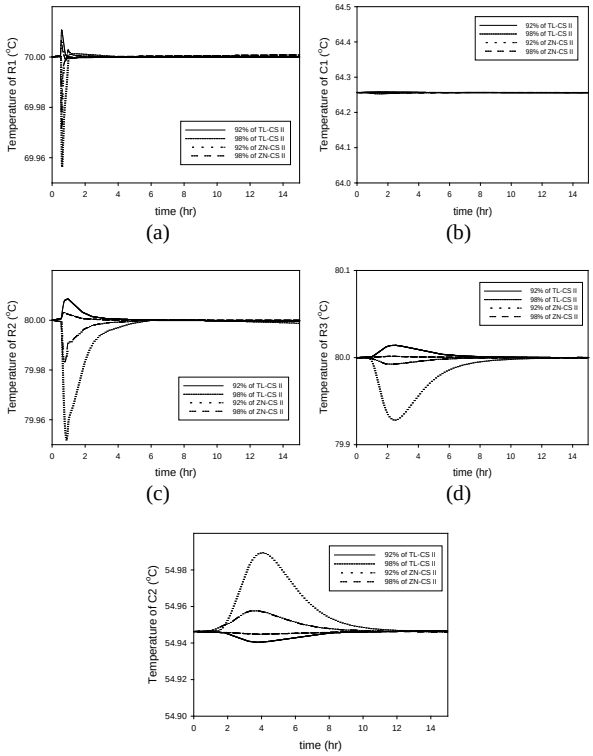

Figure 10. Temperature dynamic responses of TL and ZN-tuned control structure I for FFA in PFAD change

Table 4. RAE of control loop testing.

Testing		RAE			
		CS1		CS2	
		TL	ZN	TL	ZN
Feed flow rate	+10%	1369.286	1373.772	-	-
	-10%	942.519	941.392	-	-
Production rate	+10%	-	-	1020.918	1019.358
	-10%	-	-	843.450	842.171
Temperature	+10°C	38.524	38.622	10.435	10.742
	-10°C	53.367	53.553	15.398	15.259
Feed composition	98% FFA	552.831	552.397	613.085	611.944
	92% FFA	68.869	68.821	78.533	78.392

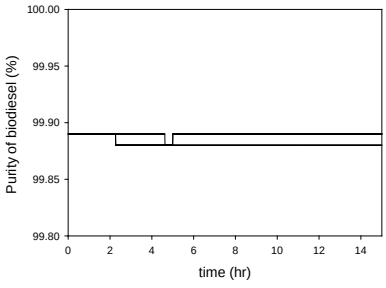

Figure 11. Purity of biodiesel of all robustness tested.

biodiesel standard. The purity of biodiesel of entire testes had similar results as shown in Figure 11. The 5th stage of both distillation columns that could be used as the temperature control tray was able to handle the methanol composition in recycle stream over 99.5 weight%.

4. Conclusions

Biodiesel production from PFAD which was a byproduct of crude palm oil refining had been evaluated. The kinetic modeling obeyed a pseudo-first order for forward reaction and second order for backward reaction that provided a good fit with experimental values. The production process was simulated. Conventional and on-demand control structures were proposed that could reject disturbance and set point change.

Acknowledgements

This work was supported by Prince of Songkla scholarship, Graduate School, Prince of Songkla University; the Specialized R&D Center for Alternative Energy from Palm Oil and Oil Crops, Thailand.

References

Aspen Technology Inc. (2008). Aspen plus biodiesel model. Bedford, MA: Author.

Chongkhong, S., Tongurai, C., Chetpattananondh, P., & Bunyakan, C. (2007). Biodiesel production by esterification of palm fatty acid distillate. *Biomass and Bioenergy, 31*, 563–568.

Fogler, H. S. (2008). *Elements of chemical reaction engineering*. London, England: Pearson Education, Inc.

Hung, S. B., Chen, J. H., Lin, Y. D., Huang, H. P., Lee, M. J., Ward, J.D., & Yu, C. C. (2010). Control of plantwide reactive distillation processes: Hydrolysis, transesterification and two-stage esterification. *Journal of the Taiwan Institute of Chemical Engineers, 41*, 382–402.

Issariyakul, T., & Dalai, A.K. (2012). Comparative kinetics of transesterification for biodiesel production from palm oil and mustard oil. *The Canadian Journal of Chemical Engineering, 90*, 342–350.

Jain, S., Sharma, M. P., & Rajvanshi, S. (2011). Acid base catalyzed transesterification kinetics of waste cooking oil. *Fuel Processing Technology, 92*, 32–38.

Kapilakarn, K., & Peugtong, A. (2007). A comparison of costs of biodiesel production from transesterification. *International Energy Journal, 8*, 1–6.

Khan, M. A., Yusup, S., & Ahmad, M. M. (2010). Acid esterification of a high free fatty acid crude palm oil and crude rubber seed oil blend: *Optimization and parametric analysis. Biomass and Bioenergy, 34*, 1751–1756.

Lamaisri, C., Punsuvon, V., Chanprame, S., Arunyanark, A., Srinives, P., & Liangsakul, P. (2015). Relationship between fatty acid composition and biodiesel quality for nine commercial palm oils.

Songklanakarin Journal of Science and Technology, 37, 389–395.

Luyben, W. L. (2002). *Plantwide dynamic simulators in chemical processing and control.* New York, NY: Marcel Dekker.

Luyben, W. L. (2006). Evaluation of criteria for selecting temperature control trays in distillation columns. *Journal of Process Control, 16*, 115–134.

Luyben, W. L., & Luyben, M. L. (1998). Plantwide process control. New York, NY: McGraw-Hill.

Prasertsit, K., Mueanmas, C., & Tongurai, C. (2013). Transesterification of palm oil with methanol in a reactive distillation column. *Chemical Engineering and Processing: Process Intensification, 70*, 21–26.

Prasertsit, K., Phoosakul, P., & Sukmanee, S. (2014). Use of calcium oxide in palm oil methyl ester production. *Songklanakarin Journal of Science and Technology, 36*, 195–200.

Shen, Y. H., Cheng, J. K., Ward, J. D., & Yu, C. C. (2011). Design and control of biodiesel production processes with phase split and recycle in the reactor system. *Journal of the Taiwan Institute of Chemical Engineers, 42*, 741–750.

Simasatitkul, L., Arpornwichanop, A., & Gani, R. (2013). Design methodology for bio-based processing: Biodiesel and fatty alcohol production. *Computers and Chemical Engineering, 57*, 48–62.

The American Oil Chemists' Society. (1997). *Official methods and recommended practices of the AOCS Ca 5a-40.* Urbana, IL, Author.

Van Gerpen, J., Shanks, B., Pruszko, R., Clements, D., & Knothe, G. (2004). *Biodiesel production technology.* Golden, CO: National Renewable Energy Laboratory.

Wenzel, B., Tait, M., Módenes, A., & Kroumov, A. (2006). Modelling chemical kinetics of soybean oil transesterification process for biodiesel production: An analysis of molar ratio between alcohol and soybean oil temperature changes on the process conversion rate. *Bioautomation, 5*, 13–22.

West, A. H., Posarac, D., & Ellis, N. (2008). Assessment of four biodiesel production processes using HYSYS. plant. *Bioresource Technology, 99*, 6587–6601.

Yadav, P. K. S., Singh, O., & Singh, R. P. (2010). Palm fatty acid biodiesel: Process optimization and study of reaction kinetics. *Journal of Oleo Science, 59*, 575–580.

Zhang, Y., Dubé, M. A., McLean, D. D., & Kates, M. (2003). Biodiesel production from waste cooking oil: 1. Process design and technological assessment. *Bioresource Technology, 89*, 1–16.